Journal of Applied Sciences and Nanotechnology, Vol. 2, No. 3 (2022)

Journal of Applied Sciences and Nanotechnology

Journal homepage: https://jasn.uotechnology.edu.iq/

Chitosan/PVA/PEG Blend Strengthened with MgO Nanoparticles for Antibacterial Application

[1]Ishraq A. Fadhil*, [2]Balqees M. Aldabbagh, [3]Wijdan T. Mahdi

[1]Department of Physics, College of Education, University of Al-Qadisiyah – Iraq

[2]Materials Science Division, Department of Applied Sciences, University of Technology – Iraq

[3]Department of Biology, College of Science, University of Al-Qadisiyah – Iraq

Article information

Article history:
Received: December, 23, 2021
Accepted: March, 16, 2022
Available online: September, 10, 2022

Keywords:
Hydrogel,
Antibacterial activity,
Inhibition zone,
Gram positive bacteria,
Gram negative bacteria

Corresponding Author:
Ishraq A. Fadhil
as.18.50@grad.uotechnology.edu.iq

Abstract

Chitosan holds net ionic positive charges, which contribute its ability to chemically bind with negatively charged fats, lipids, metal ions, proteins, and microorganisms. Magnesium oxide (MgO) nanoparticles are important inorganic materials with a wide band-gap used in many applications such as catalysts, antibacterial and medical products. The aim of this study was to investigate the effect of Chitosan (CHT) hydrogel loaded MgO nanoparticles on the bacterial growth. CHT/ poly vinyl alcohol (PVA)/ poly ethylene glycol (PEG) hydrogel was blended with various amounts of MgO nanoparticles. The surface morphology of the obtained blends was investigated by Field Emission Scanning Electron Microscope (FE-SEM). Evidently, surfaces with appropriate roughness were obtained for most of the prepared hydrogels. Fourier Transform Infrared Spectroscopy (FT-IR) and Energy Dispersive X-Ray analysis (EDX) were also included in this paper. Thermal properties of all samples was studied by DSC-TGA curves. The antibacterial activity of the prepared hybrids CHT/PVA/PEG/MgO nanoparticles have performed against gram positive bacteria Staphylococcus aureus (S.aureus) and Streptococcus, as well as gram negative bacteria Pseudomonas aeruginosa (P. aeruginosa) and Escherichia coli (E.coli). In this study, MgO nanoparticles various proportions presented high efficiency towards gram positive microorganisms. High resistance of gram negative bacteria against the final products was extremely detected according to measured inhibition zones which were between (0-9) mm.

DOI: 10.53293/jasn.2022.4552.1123, Department of Applied Sciences, University of Technology

1. Introduction

An integration of inorganic-organic, inorganic-inorganic, and organic-organic materials is adopted to fabricate hybrid composites, recently. Utilizing of natural polymers like chitosan loaded inorganic metals or metal oxides nanoparticles has attracted the attention of researchers to engineer hybrid composites [1]. Chitosan is a natural positive charged polysaccharide [2], which attracts researchers' interests due to its unique properties including biocompatibility, biodegradability, non-toxicity, hydrophilicity, and anti-bacterial activity [3-8]. These

characteristics have made chitosan a particularly beneficial compound in a wide range of applications, for instance, medical, chemical, environmental and agricultural fields, [9] as well as, in wound healing biomaterials, and chelating factor due to its capability to combine with proteins, cholesterol, fats, and metal ions [10]. Chitosan has a rigid crystalline structure owing to intra-molecular and inter-molecular hydrogen bonding which introduces its polymorphism [11]. Chitosan is unsolvable in many solvents but is soluble in dilute organic acids, for example, acetic acid, succinic, formic, lactic acids of pH < 6.0 due to primary amino groups on chitosan backbone which considerably produce a strong base [12]. Blended polymers fabrication has become one of the convenient methods used to provide polymeric materials with desired properties for practical applications. In particular, chitosan blended with (PVA) has been stated to have good mechanical and chemical properties, [13] through hydrophobic branch chain aggregation and hydrogen bonds formation [14]. (PEG) has also been widely utilized because of its biocompatibility and non- toxicity. Chitosan/PEG hydrogel can swell significantly due to alterations in the pH of the medium and as response to the positive charges on the network [15]. Hydrogels are formed by polymer networks of cross-linked sides that have an excessive amount of hydrophilic functional groups with affinity for water [16, 17]. Many diseases like lung infections, gingivitis, and otitis media can be resulted from various bacterial pathogens. Nanomaterials have the ability to struggle bacterial growth. Resistance development of bacteria can be inhibited by several antibiotics encapsulation techniques within nanomaterials [18-20]. Antibacterial drugs applied to infectious region through nanomaterials enhance driving the medication to the diseased cells with low side effects to sick people. High molecular weight CHT and low molecular weight CHT doped nanomaterials have presented high efficiency in combating gram-positive and gram-negative bacteria, respectively [21, 22]. Chitosan antimicrobial activity involves two main mechanisms. The first mechanism expected that cations on chitosan chains could bind with negative charges at the bacterial cell wall, which affect permeability and lead to penetrate outside solutes inside the cells. The second explanation suggested that it could interact with Deoxyribonucleic acid (DNA) of bacterial cell and then prevent Ribonucleic acid (RNA) synthesis [23]. In this work, CHT nanopowder/ PVA/ PEG hydrogels were hybridized with different weights of nanosized magnesium oxide MgO powder. FT-IR spectrum, FE-SEM, EDX, DSC-TGA analysis, and antibacterial efficiency were collected to study the active functional groups, surface morphology, thermal stability, and bacterial lethal efficiency of the blends.

2. Experimental Procedure

2.1. Materials

Chitosan nanopowder which produced by Micxy Chemical Co. with a degree of deacetylation (DD) of 95.7% and about 80 nm particles size was used. PVA (average molecular weight is 67000 g mol^{-1}) and PEG (average molecular weight is 3500 g mol^{-1}) were also utilized as plasticizer polymers. MgO nanoparticles (<50 nm) with high purity >99% were bought from Chinese source. Acetic acid glacial (extra pure/ MW. 60 g mol^{-1}) produced by Tomas Baker/India also used as solvent with chitosan. Distilled water was required as solvent and for cleaning the used tools. Gram positive and gram negative species of (*S.aureus*, *Streptococcus*), and (*P. aeruginosa*, *E.coli*), respectively are selected to examine the antibacterial effect of the prepared samples.

2.2. Preparation of the Main Polymeric Solutions

Separated steps were followed to prepare CHT, PVA and PEG solutions, firstly. 1.5g of chitosan nanopowder was dissolved in 100ml distilled water with the addition of 2ml acetic acid (2% concentration) which is a good solvent for chitosan. The mixture was well stirred at room temperature and moderate speed for about 30 min by using a magnetic stirrer. A clear and homogeneous solution that optically seen and kept away into a sealed container. 5g of each PVA and PEG polymers were dissolved into 100ml distilled water, individually. To produce a 5% concentration of each agent; the PVA solution was prepared at 80°C for 15min stirring, whereas PEG solution was mixed by a sonicator bath at room temperature for 5min and then saved into sealed containers.

2.3. Hydrogel Synthesis

In this study, CHT/PVA/PEG doped MgO nanoparticles were blended to investigate their role as antibacterial product. A sensitive electronic balance was used to measure various amounts of MgO (0.04, 0.06, and 0.08) g. Put (0.04g) of MgO in a plastic beaker and then adding (1ml) of PVA solution with well shaking by magnetic stirrer for (1min), next that, (1ml) of PEG solution poured to the mixture with continuous stirring for (1min), also. When a clear white blend was observed, (5ml) of the previously prepared chitosan was gradually added (drop by drop)

by a burette and the final product was left under continuous stirring for (30 min). The same steps were exactly managed for the two other amounts of MgO. Three individual hydrogel samples were kept into open tubes to let them dry at room temperature for a week. Semi-gel appeared at the end of the week and then dividing each sample into small specimens for characterization analyses. FE-SEM, EDX, FT-IR, DSC-TGA and antibacterial results were accomplished.

2.4. Thermogravimetric Analysis (DSC-TGA)

DSC-TGA analyses were carried out with a Universal V4.5A instrument by applying Ramp method. Approximately, (3-6) mg of provided samples were dual cured within (25-800) ºC in air at 20 ºC/min heating rate.

2.5. Incubation of the Selected Bacteria

The antibacterial activities of the prepared gels were investigated against *E.coli*, *P.aeruginosa*, *S.aureus*, and *Streptococcus* microorganisms. A 100 µl of culture suspension of the tested bacteria, roughly 10^6 CFU (colony forming units), was dispersed onto agar surface. Well diffusion method on Mueller Hinton agar (MHA) was employed to examine the microorganism growth. Concerning the antibacterial activity of the produced samples, 500 µl of each gel was put into wells of (6 mm depth, 6 mm diameter) previously made on the agar. Inhibition zones were shown after 24 h at 37 °C of incubation conditions. The growth of bacteria around wells was recorded according to the diameter of inhibition zones. Inhibition zone is the area surrounding the wells that filled by the prepared samples with different zone diameters depending on the antimicrobial efficiency.

3. Results and Discussion

3.1. FT-IR analysis

The FT-IR spectra were obtained within the range of 400–4000 cm^{-1}, but the major fingerprints of the tested samples, as shown in Figure 1, are between (1000–3345) cm^{-1}. The infrared spectrum of pure chitosan (Figure 1) reveals around 894 cm^{-1} and 1159cm^{-1} peaks pointed to saccharine structure, and a weaker amino characteristic peak appears at around 1597cm^{-1}. The peak at 1260cm^{-1} is the absorption of δ (O−H) refers to bending state, and the weak band at 1381cm^{-1} has been assigned to the -CH_3 symmetrical deformation mode. The broad characteristic peak in the region 3100–3600 cm^{-1}, related to the stretching vibration of –CH, –NH_2 and –OH bonds. The peaks at 1640 cm^{-1} for –NH_2 and 1597cm^{-1} for−OH are signed to bending vibrations on CHT backbone [24]. PVA scheme (Figure 1) shows transmittance bands at 2937, 1439, 1257, 1092 and 843 cm^{-1}, which are assigned the U_a (CH_2) asymmetric stretching, δ(CH−OH) symmetric bending mode, γ_w(CH) wagging mode, U(C−O), and U(C−C) resonance, respectively [25]. Finally, the wide recognized band around 3421cm^{-1} was due to the stretching vibration of O-H bonded to N-H [26]. The characteristic band at 1100 cm^{-1} of PEG (Figure 1) was attributed to the bending vibration of C-O, and sharp bands at 2900 related to asymmetric stretching vibration of sp^3 C-H [24].

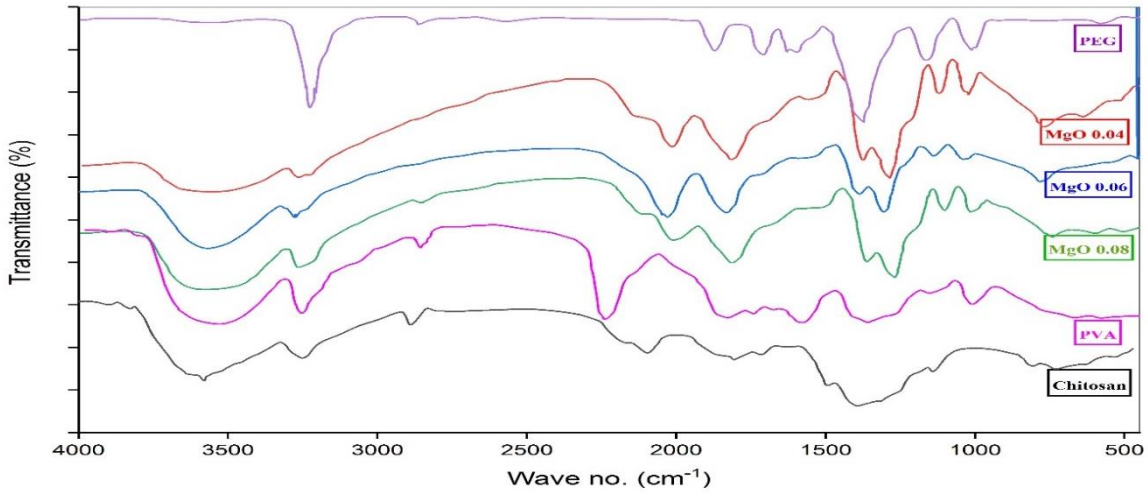

Figure 1: FTIR schemes for pure CHT, PVA, PEG, (0.04g, 0.06g, 0.08g) MgO nanocomposite hybrids.

The disappearance of crystallization sensitive bands of pure chitosan at 1078 cm^{-1} in the blends (Figure 1) implying that an intermolecular interaction between PVA/PEG with CHT disrupts the crystallinity of chitosan at the blend status, and also a wide-deep band around 3500 cm^{-1} related to the stretching vibration of amine and –OH groups with implicit –CH (sp^2) bonding [24]. CHT/ PVA/ PEG/ MgO hybrids (Figure 1) were showed broad percentage transmittances greater than 3300 cm^{-1} due to the stretching vibrations of the O–H and N–H bonds. For hybrid CHT, all the composites showed higher percentage transmittances at wavenumbers below 2000 cm^{-1} compared with the pure chitosan. The peak at 2857cm^{-1}, symmetric stretching of C–H in pure CHT, was doublet in MgO/CHT blends nearby to the first one at about 2940cm^{-1} referring to asymmetric C-H stretching bond. OH and $–NH_2$ stretching mode at (3360-3500) cm^{-1} appeared wider and less intensity than that at the spectrum of pure CHT. –OH bending mode on the CHT backbone has shifted to lower frequencies around (1565- 1573) cm^{-1} for patterns (E, F, and G) as it can be bonded with Mg^{+2}. Moreover, the appearance of peaks around 850 and 925 cm^{-1} on the spectrum of CHT/Mg gels is a characteristics of the stretching vibrations of Mg–O and Mg–N with different intensities [27].

3.2. FE-SEM/ EDX analysis

SEM is a valuable tool to evaluate the scaffold characteristics (pores, particles size, and surface morphology) of prepared hydrogels. Figure 2(A, B, C) shows the FE-SEM micrographs from the hydrogel CHT/PVA/PEG loaded (0.04, 0.06, 0.08) g of MgO nanoparticles, respectively. Images A and C display porous surfaces with many encapsulated features related to ability of chitosan for wrapping when cross-linked with PVA and PEG polymers. However, image B did not show porous micro-structures, but it shows, to some extent, a smooth texture with granular shapes instead. This probably due to the prepared blend homogeneity or due to formation of H-bonds, which led to the irregular polarity in the internal system [28]. This reason is in agreement with the results obtained from FT-IR patterns in Figure F and EDX peaks in Figure 3. Herein, it could be observed that samples of well-developed open pores can facilitate mass transfer of loaded nanoparticles for particular applications, [29] as it will be evidenced in the next section.

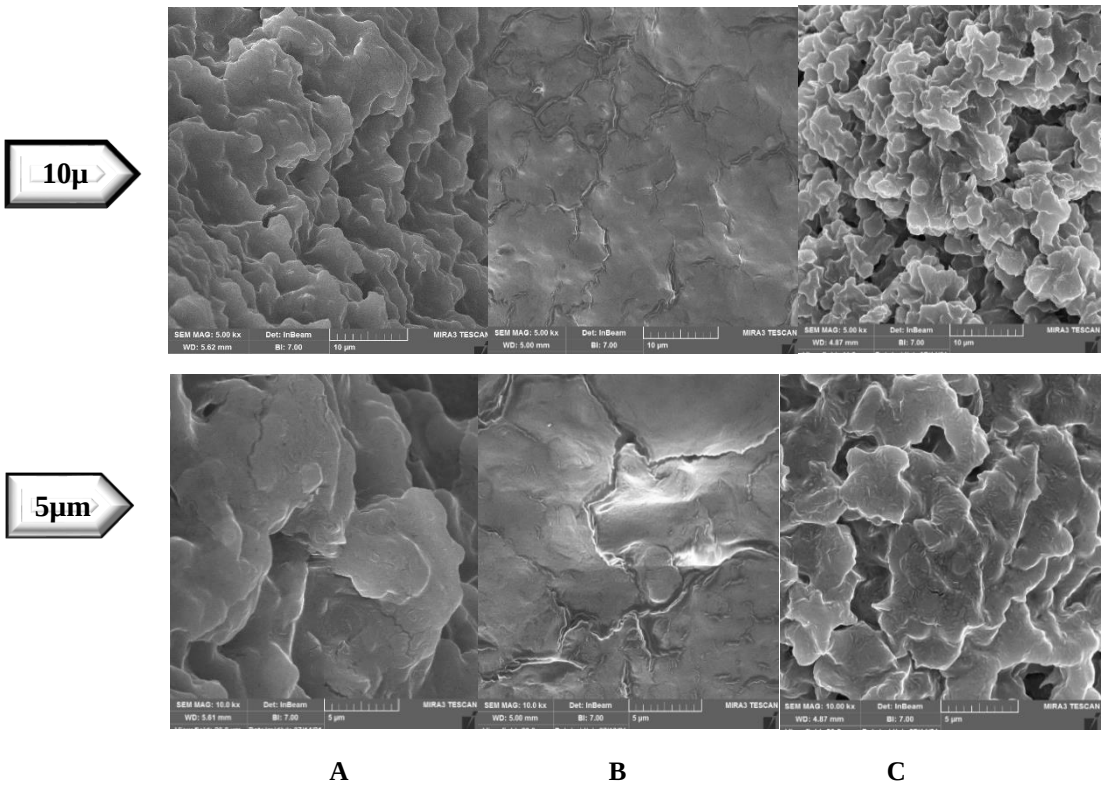

Figure 2 (A, B, C): FE-SEM images with two magnification powers (10 and 5)µm to clarify the differences among all samples morphologies such as pores, features size and shape, and grain formation, etc. related to CHT blends with (0.04, 0.06, 0.08) g of MgO nanopowder, respectively.

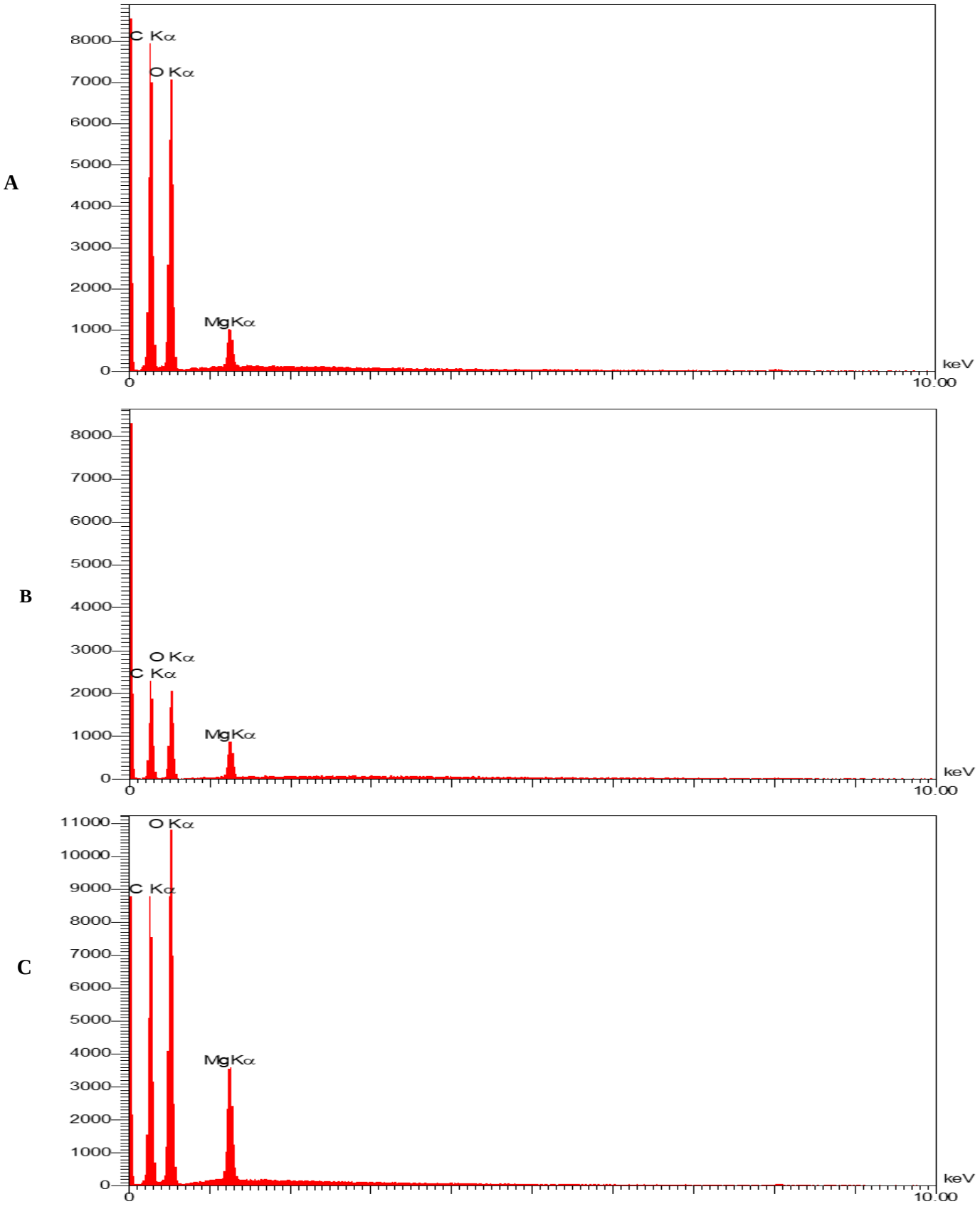

Figure 3 (A, B, C) EDX spectra of CHT hybrid materials for (0.04, 0.06, and 0.08) g of MgO nanoparticles, respectively. It demonstrates diverse concentrations of (C, O, Mg) elements in the scanned areas.

3.4. Thermal Properties of the Hydrogels

Thermogravimetric analyses TGA of the three prepared hydrogels were relied to study their thermal stability, as shown in Figure 4. The three tested composites of CHT/ PVA/ PEG/ MgO (0.04, 0.06, and 0.08) g showed a significant weight change of about 5% between (25-160) ºC, which could be proportional to evaporate the residual moisture included in the hybrids network as agree with other research studies [30, 31]. The thermal degradation started at higher temperatures due to weight loss over time. The first two diagrams (A, B) showed fairly same three stages of decomposition process appeared at about (220, 340, and 470) ºC with an approximate weight remain of (0.8-1) g at the end of this stage, respectively. For the third diagram (C), the three steps are still observed but with a notable shifting to higher temperatures. The new thermal behavior could be an indication that increasing MgO amount to 0.08g led to rise the degradation point to around 550 ºC with great ratio of remaining weight 52% wt. The previous important degradation steps can be attributed to dehydration, deacetylation, depolymerisation of utilized polymers [32], and MgO nanopowder decomposition. An obvious decrease in weight loss was detected in CHT/ PVA/ PEG/ MgO nanocomposite hydrogels with increasing MgO nanopowder quantity. It is an indication of improving their thermal stability to be optimal antimicrobial and medical products [33].

A

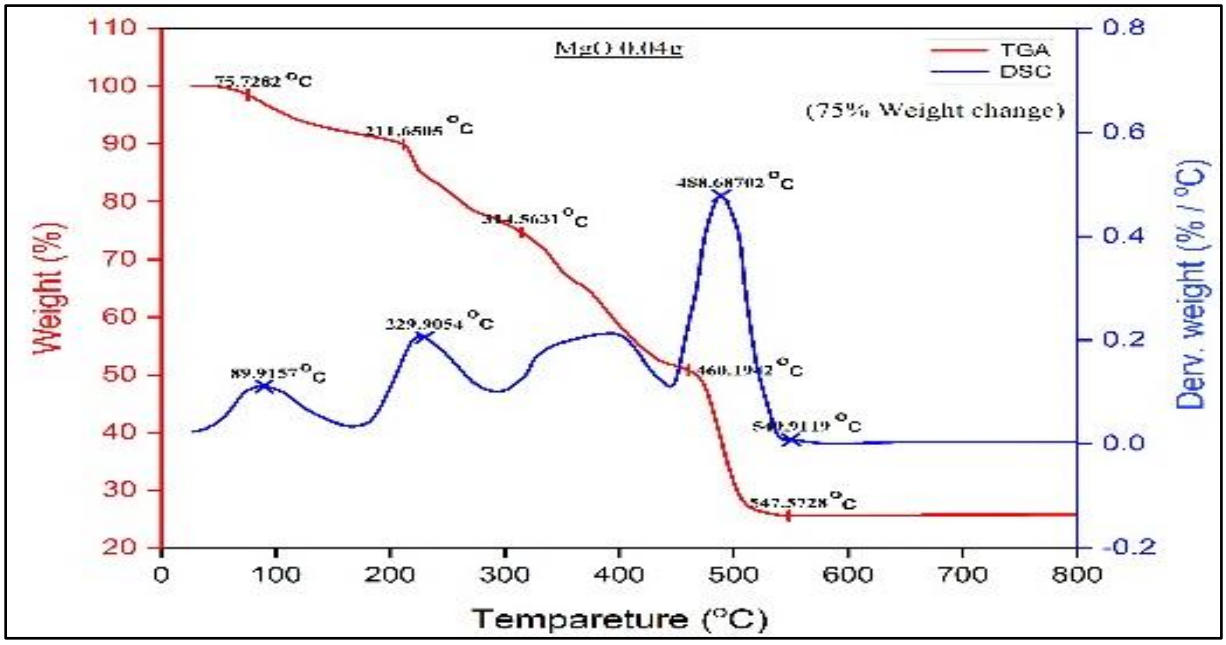

B

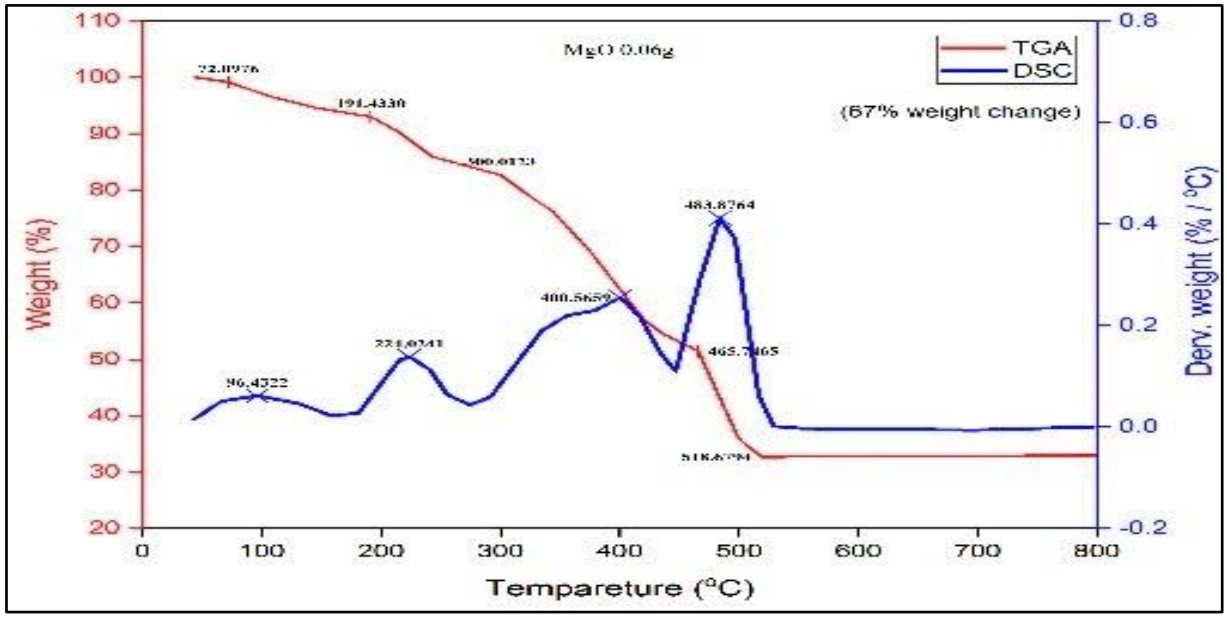

C

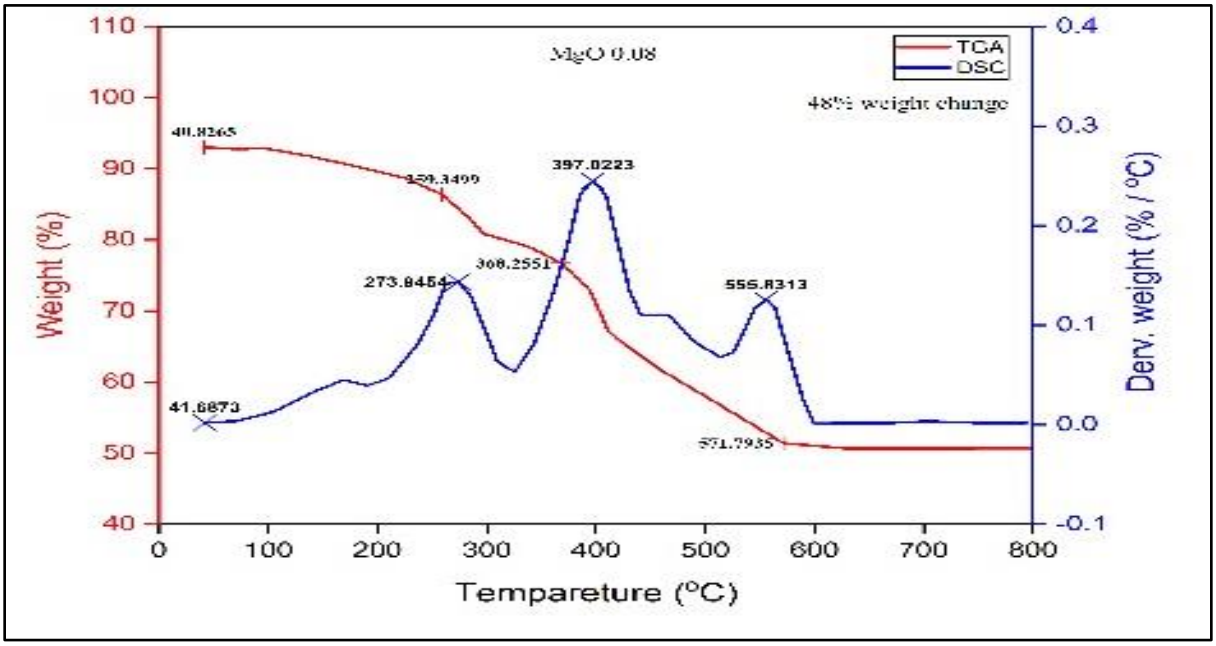

Figure 4 (A, B, C) DSC-TGA curves of the three prepared composites of CHT/ PVA/ PEG/ MgO (0.04, 0.06, 0.08) g, respectively.

3.5. Bacterial Investigations

The antibacterial assay of the prepared nanocomposites is stated in Figure 5 and Table 1. Figure 5 showed remarkable changes in the diameter of the inhibition zones surrounding the determined wells. This may be related to the ability of CHT blend and MgO nanoparticles in attacking cell-walls of the bacteria and restricting their activity. It is well known that chitosan has tremendous metal-binding abilities, where amino charged groups interact with metals [34]. The interaction between amino groups and divalent ions like Mg^{2+} prevents the production of toxins and inhibits bacterial growth [35]. The antibacterial effect of MgO may result a damage to the peptide linkages at super-oxide ions on the carbonyl group, which causes degradation the protein of the pathogens. MgO reacts with intracellular oxygen to create reactive oxygen species ROS such as $O_2^{\bullet-}$, $OH^{\bullet}$ and H_2O_2 which could be delivered into the medium [36] and then motivates the destructive efficiency towards the bacterial cell wall [37].

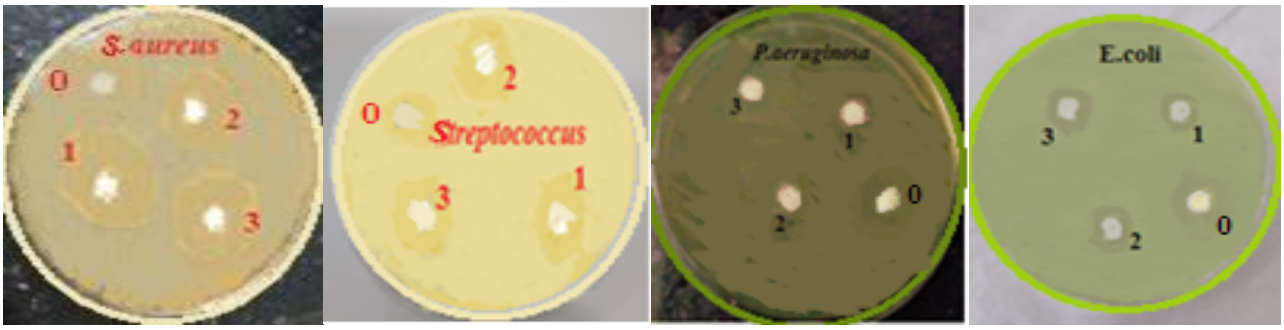

Figure 5: photographs of antimicrobial activity for *S.aureus* and *Streptococcus (gram positive pathogens), P.aeruginosa and E.coli (gram negative pathogens,* which display the variety of inhibition zones diameters as a function of MgO weight and bacteria type.

The results revealed that the CHT hybridized with polymeric agents and MgO nanopowder did not exhibit a significant antibacterial efficiency against gram negative strains as compared with gram positive ones. Thereby, slightly inconsiderable inhibition zones for all tested samples against *P.aeruginosa and E.coli* between (0-9) mm

were observed. In agreement with Bindhu, et al. (2014) who reported that MgO nanoparticles exhibited high efficiency against gram positive than the gram negative microorganisms. This behavior may be related to the susceptibility differences of various grown bacteria tested in this work [38, 39]. Principally, gram-positive bacteria have a single lipid bilayer (monoderms), whereas gram-negative bacteria have two bilayers (diderms) [40]. Generally, nanoparticles could penetrate the cell wall by either diffusion through the cell membrane or inserting into the nucleus which cause mitosis as the membrane dissolves during this process [41]. The fluctuated values of measured diameters of the inhibition zones for the prepared hybrids, as appeared in Table 1, could be also attributed to various surface morphology of examined samples. As shown in Figure 2, major characteristic structures such as: pores, size and shape of features, distribution of MgO nanoparticles along the active area, cracks, and bulk grains formation may have a significant role in the antibacterial mechanism.

Table 1: the results of the inhibition zones diameters measured for four types of common bacteria with diverse MgO amounts into the prepared hybrids; where S_0: the control sample (zero MgO), S_1: 0.04g MgO, S_2: 0.06g MgO, S_3: 0.08g MgO.

Samples	*S.aureus* (mm)	*Streptococcus* (mm)	*P.aeruginosa* (mm)	*E.coli* (mm)
S_0	21	10	8	9
S_1	40	14	0	3
S_2	35	15	0	4
S_3	38	14	0	5

4. Conclusions

Blended hydrogel samples of CHT/PVA/PEG with various proportions of MgO nanoparticles were prepared. Investigation of the surface morphology of the obtained blends displayed good porous texture for only two MgO concentrations (0.04 and 0.08) g, while the last sample showed a smooth and bulk grains surface as revealed by the results of FE-SEM images. From FT-IR schemes, disappearance of bending amino band for 0.06g MgO sample may reflect the lack of its antibacterial effect, and its non-porosity could be explained due to the intermolecular hydrogen bonding existing between the amino groups of chitosan and the hydroxyl groups of PVA/PEG. The antibacterial activity of the prepared hybrids have executed against gram positive bacteria (*S.aureus, Streptococcus)* and gram negative bacteria (*P.aeruginosa, E.coli)*. In this study, the added MgO nanoparticles performed more efficient against gram positive microorganisms than the other type gram negative. The differences observed in the diameter of inhibition zone may be due to the variation in the susceptibility of diverse pathogens to the prepared nanoparticles. Characteristically, gram positive bacteria have no external membrane in the cell wall. Otherwise, gram-negative bacteria have more complex cell wall structure with an interfacial layer of peptidoglycan between outer and cytoplasmic membranes. Accordingly, the cell wall of gram positive bacteria can be easily degraded. The antibacterial efficiency of CHT/MgO nanoparticles gel may be also responsible to the binding of surface oxide ion to the bacteria and depends on the available surface area for interaction.

Acknowledgement

We gratefully thank and appreciate the efforts of staff at the Department of Applied Sciences/ the University of Technology- Iraq. The authors are responsible for their funding support.

Conflict of Interest

We (the authors) declare that we have no conflict of interest.

References

[1] L. M. Anaya-Esparza, “Effect of Mixed Oxide-Based TiO2 on the Physicochemical Properties of Chitosan Films”, *Period. Polytech. Chem. Eng.*, 2022.

[2] M. Abdulkareem, A. Abdalsalam and A. Bohan, "Influence of chitosan on the antibacterial activity of composite coating (PEEK /HAp) fabricated by electrophoretic deposition", *Progress in Organic Coatings*, vol. 130, pp. 251-259, 2019.

[3] Y. Shigemasa and S. Minami, "Applications of Chitin and Chitosan for Biomaterials", *Biotechnology and Genetic Engineering Reviews*, vol. 13, no. 1, pp. 383-420, 1996.

[4] I. van der Lubben, J. Verhoef, G. Borchard and H. Junginger,"Chitosan for mucosal vaccination", *Advanced Drug Delivery Reviews*, vol. 52, no. 2, pp. 139-144, 2001.

[5] Y. Dong, W. Qiu, Y. Ruan, Y. Wu, M. Wang and C. Xu, "Influence of Molecular Weight on Critical Concentration of Chitosan/Formic Acid Liquid Crystalline Solution", *Polymer Journal*, vol. 33, no. 5, pp. 387-389, 2001.

[6] I. Henriksen, Ø. Skaugrud and J. Karlsen, "Use of chitosan and chitosan malate as an excipient in wet granulation of three water soluble drugs", *International Journal of Pharmaceutics*, vol. 98, no. 1-3, pp. 181-188, 1993.

[7] H. Hamedi, S. Moradi, S. Hudson and A. Tonelli, "Chitosan based hydrogels and their applications for drug delivery in wound dressings: A review", *Carbohydrate Polymers*, vol. 199, pp. 445-460, 2018.

[8] G. Payne, W. Sun and A. Sohrabi, "Tyrosinase reaction/chitosan adsorption for selectively removing phenols from aqueous mixtures", *Biotechnology and Bioengineering*, vol. 40, no. 9, pp. 1011-1018, 1992.

[9] E. El-Hefian, M. Nasef, A. Yahaya and R. Khan, "Preparation and Characterization of Chitosan/Agar Blends: Rheological and Thermal Studies", *Journal of the Chilean Chemical Society*, vol. 55, no. 1, 2010.

[10] H. M. Ibrahim, and E. M. R. El-Zairy. "Chitosan as a biomaterial—structure, properties, and electrospun nanofibers", *Concepts, compounds and the alternatives of antibacterials* (2015): 81-101.

[11] Q. Li, E. Dunn, E. Grandmaison and M. Goosen, "Applications and Properties of Chitosan", *Journal of Bioactive and Compatible Polymers*, vol. 7, no. 4, pp. 370-397, 1992.

[12] A. Shakeel, M. Ahmad, and S. Ikram. "Chitosan: a natural antimicrobial agent-a review." *Journal of Applicable Chemistry*, vol. 3, no. 2, pp. 493-503, (2014).

[13] A. Rajeswari, A. Amalraj and A. Pius, "Adsorption studies for the removal of nitrate using chitosan/PEG and chitosan/PVA polymer composites", *Journal of Water Process Engineering*, vol. 9, pp. 123-134, 2016.

[14] N. Suyatma, L. Tighzert, A. Copinet and V. Coma, "Effects of Hydrophilic Plasticizers on Mechanical, Thermal, and Surface Properties of Chitosan Films", *Journal of Agricultural and Food Chemistry*, vol. 53, no. 10, pp. 3950-3957, 2005.

[15] X. Xu, B. Gao, X. Tan, Q. Yue, Q. Zhong and Q. Li, "Characteristics of amine-crosslinked wheat straw and its adsorption mechanisms for phosphate and chromium (VI) removal from aqueous solution", *Carbohydrate Polymers*, vol. 84, no. 3, pp. 1054-1060, 2011.

[16] D. Algul, A. Gokce, A. Onal, E. Servet, A. Dogan Ekici and F. Yener, "In vitrorelease andIn vivobiocompatibility studies of biomimetic multilayered alginate-chitosan/β-TCP scaffold for osteochondral tissue", *Journal of Biomaterials Science, Polymer Edition*, vol. 27, no. 5, pp. 431-440, 2016.

[17] A. Koç, G. Finkenzeller, A. Elçin, G. Stark and Y. Elçin, "Evaluation of adenoviral vascular endothelial growth factor-activated chitosan/hydroxyapatite scaffold for engineering vascularized bone tissue using human osteoblasts: In vitro and in vivo studies", *Journal of Biomaterials Applications*, vol. 29, no. 5, pp. 748-760, 2014.

[18] Anwar Sabri Jawad, Qasim Najem Obaid Thewaini, Sharafaldin Al-Musawi, "Cytotoxicity Effect and Antibacterial Activity of Al2O3 Nanoparticles Activity against Streptococcus Pyogenes and Proteus Vulgaris", *Journal of Applied Sciences and Nanotechnology*, vol. 1, pp. 3, 2021.

[19] R. A. Jabbar, N. N. Hussein, Evaluation The Antibacterial Activity of Biosynthesis Silver Nanoparticles by Lactobacillus Gasseri Bacteria, *Journal of Applied Sciences and Nanotechnology*, vol. 1, no. 3, pp. 86-95, 2021

[20] A. Jawad, Q. Thewaini and S. Al-Musawi, "Cytotoxicity Effect and Antibacterial Activity of Al2O3 Nanoparticles Activity against Streptococcus Pyogenes and Proteus Vulgaris", *Journal of Applied Sciences and Nanotechnology*, vol. 1, no. 3, pp. 42-50, 2021.

[21] M. Yeh, W. Chang, Y. Tai, C. Chiang, C. Hu and Po-da Hong, "The comparison of protein-entrapped liposomes and lipoparticles: preparation, characterization, and efficacy of cellular uptake", *International Journal of Nanomedicine*, p. 2403, 2011.

[22] F. Tamara, C. Lin, F. Mi and Y. Ho, "Antibacterial Effects of Chitosan/Cationic Peptide Nanoparticles", *Nanomaterials*, vol. 8, no. 2, p. 88, 2018.

[23] F. Croisier and C. Jérôme, "Chitosan-based biomaterials for tissue engineering", *European Polymer Journal*, vol. 49, no. 4, pp. 780-792, 2013.

[24] H. Zheng, Y. Du, J. Yu, R. Huang, and L. Zhang, "Preparation and characterization of chitosan/poly(vinyl alcohol) blend fibers," *Journal of Applied Polymer Science*, vol. 80, no. 13, pp. 2558–2565, 2001.

[25] S. Krimm, C. Y. Liang, and G. B. Sutherland, "Infrared spectra of high polymers. V. POLYVINYL ALCOHOL," *Journal of Polymer Science*, vol. 22, no. 101, pp. 227–247, 1956.

[26] Q. Wang, N. Zhang, X. Hu, J. Yang, and Y. Du, "Chitosan/polyethylene glycol blend fibers and their properties for drug controlled release," *Journal of Biomedical Materials Research Part A*, vol. 85A, no. 4, pp. 881–887, 2008.

[27] M. Yazdani, E. Virolainen, K. Conley, and R. Vahala, "Chitosan–Zinc(II) complexes as A Bio-Sorbent for The Adsorptive abatement of Phosphate: Mechanism OF COMPLEXATION and assessment of Adsorption Performance," *Polymers*, vol. 10, no. 1, p. 25, 2017.

[28] L. Liu, Q. Gao, X. Lu, and H. Zhou, "In situ forming hydrogels based on chitosan for drug delivery and tissue regeneration," *Asian Journal of Pharmaceutical Sciences*, vol. 11, no. 6, pp. 673–683, 2016.

[29] E. Ruel-Gariépy, A. Chenite, C. Chaput, S. Guirguis, and J.-C. Leroux, "Characterization of thermosensitive chitosan gels for the sustained delivery of drugs," *International Journal of Pharmaceutics*, vol. 203, no. 1-2, pp. 89–98, 2000.

[30] P. Sautrot-Ba et al., "Paprika, Gallic Acid, and Visible Light: The Green Combination for the Synthesis of Biocide Coatings", *ACS Sustainable Chemistry & Engineering*, vol. 6, no. 1, pp. 104-109, 2017.

[31] N. TERAMOTO and M. SHIBATA, "Synthesis and properties of pullulan acetate. Thermal properties, biodegradability, and a semi-clear gel formation in organic solvents", *Carbohydrate Polymers*, vol. 63, no. 4, pp. 476-481, 2006.

[32] P. Sautrot-Ba et al., "Photoinduced chitosan–PEG hydrogels with long-term antibacterial properties", *Journal of Materials Chemistry B*, vol. 7, no. 42, pp. 6526-6538, 2019.

[33] A. Hezma, A. Rajeh and M. Mannaa, "An insight into the effect of zinc oxide nanoparticles on the structural, thermal, mechanical properties and antimicrobial activity of Cs/PVA composite", *Colloids and Surfaces A: Physicochemical and Engineering Aspects*, vol. 581, p. 123821, 2019.

[34] A. J. Varma, S. V. Deshpande, and J. F. Kennedy, "Metal complexation by chitosan and its derivatives: A review," *Carbohydrate Polymers*, vol. 55, no. 1, pp. 77–93, 2004.

[35] G. Kravanja, M. Primožič, Ž. Knez, and M. Leitgeb, "Chitosan-Based (nano) materials for Novel biomedical applications," *Molecules*, vol. 24, no. 10, p. 1960, 2019.

[36] M. Z. Baghbaderani *et al.*, "Dual Synergistic Effects of MgO-GO Fillers on Degradation Behavior, Biocompatibility and Antibacterial Activities of Chitosan Coated Mg Alloy," *Coatings*, vol. 12, no. 1, p. 63, Jan. 2022.

[37] K. Krishnamoorthy, G. Manivannan, S. J. Kim, K. Jeyasubramanian, and M. Premanathan, "Antibacterial activity of MgO nanoparticles based on lipid peroxidation by oxygen vacancy," *Journal of Nanoparticle Research*, vol. 14, no. 9, 2012.

[38] M. Bindhu and M. Umadevi, "Surface plasmon resonance optical sensor and antibacterial activities of biosynthesized silver nanoparticles", *Spectrochimica Acta Part A: Molecular and Biomolecular Spectroscopy*, vol. 121, pp. 596-604, 2014.

[39] M. Bindhu and M. Umadevi, "Antibacterial activities of green synthesized gold nanoparticles", *Materials Letters*, vol. 120, pp. 122-125, 2014.

[40] R. S. Gupta, “Origin of Diderm (gram-negative) BACTERIA: Antibiotic selection pressure rather Than Endosymbiosis likely led to the evolution of bacterial cells with two membranes,” *Antonie van Leeuwenhoek*, vol. 100, no. 2, pp. 171–182, 2011.

[41] I. Fadhil, "Investigation of USPION genotoxicity on Cytokinesis Blocked Micronuclei", *International Journal of Pharmaceutical Research*, vol. 11, no. 02, pp. 115-120, 2019.